The dynamics of small excitable ion channel clusters

J.W. Shuai
Department of Neurobiology and Behavior, University of California, Irvine, California 92697

P. Jung
Department of Physics and Astronomy and Quantitative Biology Institute, Ohio University, Athens, Ohio 45701

(Received 1 February 2006; accepted 13 May 2006; published online 30 June 2006)

Through computational modeling we predict that small sodium ion channel clusters on small patches of membrane can encode electric signals most efficiently at certain magic cluster sizes. We show that this effect can be traced back to algebraic features of small integers and are universal for channels with a simple gating dynamics. We further explore physiologic conditions under which such effects can occur. © *2006 American Institute of Physics*. [DOI: 10.1063/1.2210827]

Ion channel clustering is an often observed but poorly understood phenomenon. Mathematical modeling is an excellent tool to explore the behavior of clustered ion channels. Clusters of excitable channels give rise to fluctuations in the membrane potential which are inversely proportional to the cluster size if the clusters are comprised of a large—but not infinite—number of ion channels. In recent literature, the relation between cluster size and fluctuations has led to the concept of system-size stochastic resonance and coherence resonance.[1–5] More recent work has focused on stochastic effects in ultrasmall channel clusters with 1–50 channels per cluster.[6] For clusters of such small size exponential system-size scaling of the fluctuations breaks down and novel entropic effects can be observed. At certain *magic* cluster sizes, the spontaneous rate of action potentials and signal encoding exhibits maxima. In this paper we extent our recent analysis to include a detailed discussion of the physiologic conditions under which this effect may occur and how it could be implemented in a biomimetic device. We supplement our simple microcanonical theory of the cluster entropy with more accurate statistics and discuss issues of distinguishability of channel proteins. We provide additional evidence that these maxima are caused by the discreteness of inverse small integers and resulting algebraic properties. The effect is therefore universal and does not depend on the nature of the channel and system.

I. INTRODUCTION

Ion channels are devices that allow the passage of specific ions from outside the cell to inside the cell. Their abundance determines the electric behavior of a membrane and—in the case of neurons—the cell's capability of firing an action potential. In some other cell types, like for example, astrocytes, the large abundance of potassium ion channels renders these cells buffers for potassium ions in the extracellular space.

Recently, the electric behavior of neuronal membranes with clustered ion channels has attracted increasing attention. This interest originates partially in the Biology community, where ion channel clustering is observed frequently, but the mechanism and the functional role (if any) are poorly understood. New hypotheses like impact of channel clustering on signaling functions and information coding fall on futile grounds. In some membranes, ion channel clustering is in fact a dynamical phenomenon that is regulated by the *state* of the channels,[7] further fueling the idea that clustering of ion channels is more than an epi-phenomenon. Physicists have become interested since small clusters with few channels are intrinsically stochastic and provide an ideal playground where novel ideas for the possible role of fluctuations can be tested. One main line of investigation in this area exploits the relation between channel noise and cluster size. Hence, well-known effects such as stochastic resonance[8] and coherence resonance[4,5,9] translate into system-size stochastic and coherence resonance. More recently, in another line of research, we demonstrated novel *entropic* effects in ultrasmall, excitable ion channel clusters that are due to the discrete nature of small numbers and are hence fundamental to these systems.[6] These effects surfaced in unexpected peaks and valleys of spontaneous firing rates of action potentials at certain cluster sizes and in the enhancement of encoding of weak signals.

In this paper, we will give a detailed account of these effects, discuss physiologic conditions under which they may occur by embedding the cluster into a spatially extended leaky membrane structure, and discuss the mathematical structure underlying the organization of these magic cluster sizes. In Sec. II we consider a one-dimensional infinite cable, representing an axon or dendrite, with a cluster of sodium channels. We solve the cable equations inside and outside the cluster and identify the relevant length and time scales of the system. We derive conditions under which voltage gradients can be neglected and hence conditions under which spatially nonexplicit models accurately describe the electric behavior of the cluster. The same theory determines how small a patch of membrane has to be in order for clusters with few channels can actually elicit action potentials.

In Sec. III, we place sodium channels at constant surface density on an isolated patch of membrane and consider the generation of action potentials and encoding of small current

inputs in terms of action potentials. It is shown that the spontaneous firing rate as well as the signal encoding assumes multiple maxima at magic cluster sizes. Underlying theories based on the statistical physics of the states of the ion channel clusters with distinguishable and nondistinguishable ion channels in microcanonical and other ensembles are discussed. All theories suggest that entropic effects are underlying the appearance of the magic cluster sizes.

II. SETTING THE STAGE: TIME SCALES AND LENGTH SCALES

The lipid bilayer of the cell membrane can be considered electrically as a capacitor with a small specific capacitance of approximately $\bar{C}=1\ \mu\mathrm{F/cm}^2$. The conductance (per membrane area) of the membrane is due to ion channels with ion-specific conductance (per membrane area) g_i and a nonspecific conductance (per membrane area) g_m. We consider a one-dimensional infinite cable, representing a dendrite or the axon along the x axis of a coordinate system. The membrane potential of such a system is well-characterized by the cable equation,[10,11] i.e.,

$$\bar{C}\dot{u}(x,t) = -g_m(u(x,t)-u_m) - \sum_i g_i(x,u)(u(x,t)-u_i) + \lambda^2 g_m \frac{\partial^2 u(x,t)}{\partial x^2}, \tag{1}$$

with the reversal potentials u_m and u_i. The characteristic time scale τ and length scale λ are given by

$$\tau = \frac{\bar{C}}{g_m}, \quad \lambda = \sqrt{\frac{d}{4\rho g_m}}, \tag{2}$$

where ρ denotes the specific resistance of the cable core [Ω cm]. Typically τ is of the order of a few ms while λ is of the order of a few mm. The diameter of the cable is denoted by d. The x dependence of the conductance g_i takes into account the spatial distribution of the specific ion channels. The voltage dependence of the ionic conductance are the essential nonlinearities giving rise to action potentials. The length scale λ determines the scale on which deviations from the resting voltage of the membrane change in space and hence presents a measure of the distance across which ion channels can interact through coupling by the membrane potential.

We now distribute N sodium channels onto a segment of the cable of length L_{Na} centered around $x=0$ for mathematical simplicity. We consider the channels to be smeared out continuously along the segment. When a channel is open it conducts sodium ions with a conductance of $\gamma=20$ pS. Hence, if n of the N channels are open, the conductance leads to a spatial sodium conduction profile of the form

$$g_{\mathrm{Na}}(x) = \mathrm{rect}(x, L_{\mathrm{Na}}) \frac{n\gamma_{\mathrm{Na}}}{\pi d L_{\mathrm{Na}}} \tag{3}$$

with $\mathrm{rect}(x,L)=1$ for $|x|<L/2$ and $\mathrm{rect}(x,L)=0$ otherwise. The area $\pi d L_{\mathrm{Na}}$ denotes the membrane surface area of the ion channel cluster on the cylindric axon with diameter d. The total conductance per axon circumference is given by $n\gamma_{\mathrm{Na}}/\pi d$.

We want to determine the spatial steady-state voltage profile, generated if n of the N channels are open and contribute to sodium conductance. The steady-state profile along the cable (in dimensionless variables $\hat{x}=x/\lambda$) for $|x|>L_{\mathrm{Na}}/2$ is determined by the differential equation

$$\frac{\partial^2 u}{\partial \hat{x}^2} = u - u_m \tag{4}$$

and for $|x|<L_{\mathrm{Na}}/2$ by

$$-(g_{\mathrm{Na}}+g_m)(u-u_R) + g_m \frac{\partial^2 u}{\partial \hat{x}^2} = 0 \tag{5}$$

with

$$u_R = \frac{g_m u_m + g_{\mathrm{Na}} u_{\mathrm{Na}}}{g_m + g_{\mathrm{Na}}}. \tag{6}$$

The solution of Eqs. (5) and (6) can be easily obtained by solving the linear equations for the intervals $|x|<L_{\mathrm{Na}}/2$ and $|x|>L_{\mathrm{Na}}/2$ separately and matching the voltages and their slopes at the interfaces $x=\pm L_{\mathrm{Na}}/2$. The results are

$$u = u_R - \frac{(1-\epsilon^{-2})(u_{\mathrm{Na}}-u_m)}{\cosh(\hat{l}\epsilon)+\epsilon\sinh(\hat{l}\epsilon)}\cosh(\epsilon\hat{x}) \quad \text{for } |x|<L_{\mathrm{Na}}/2,$$
$$u = u_m + \frac{(1-\epsilon^{-2})(u_{\mathrm{Na}}-u_{\mathrm{m}})}{1+\epsilon\coth(\epsilon\hat{l})}\exp(-(|\hat{x}|-\hat{l})) \quad \text{for } |x|>L_{\mathrm{Na}}/2, \tag{7}$$

with

$$\hat{l} = \frac{L_{\mathrm{Na}}}{2\lambda}, \quad \epsilon = \sqrt{1+(g_{\mathrm{Na}}/g_m)}. \tag{8}$$

In the case that all sodium channels are closed, i.e., $n=0$, the voltage profile becomes uniform $u=u_m$ (as it obviously has to be). For $n\neq 0$, the profile decays exponentially outside of the cluster ($|x|>L_{\mathrm{Na}}/2$) on the length scale λ while it is more flat inside the cluster, decaying parabolically on the length scale $\lambda\epsilon$ with $\epsilon>1$.

In order to analyze what these results mean for the voltage profile generated by the cluster of n open sodium channels along the cable, we need to insert realistic values for the parameters. Let us assume our ion channels cluster has a length of 1 μm and that the dendrite has a diameter of 2 μm. With a single channel conductance of 20 pS, we find for the sodium conductance $g_{\mathrm{Na}}=n/\pi\mathrm{mS/cm}^2$. A typical value for the membrane resistivity $r_m=10^3\ \Omega\,\mathrm{cm}^2$ leads to $g_m=1/r_m=1\ \mathrm{mS/cm}^2$. Hence, the parameter ϵ which determines in conjunction with $\lambda\approx 1$ mm the voltage profile [see Eq. (8)] is given by (for fixed cluster size)

$$\epsilon^2 = 1 + \frac{g_{\mathrm{Na}}}{g_{\mathrm{m}}} = 1 + \frac{n}{\pi}. \tag{9}$$

For a density of sodium channels according the Hodgkin-Huxley model, i.e., $\rho=60/\mu\mathrm{m}^2$, the membrane area of the cluster is $2\pi\ \mu\mathrm{m}^2$ and the cluster will be comprised of $n=377$ sodium channels. This leads to $\epsilon=11$. The voltage assumes its maximum at the center of the cluster ($x=0$) and

then falls off according to $-\cosh(x/\lambda\epsilon)$. Given that $\lambda \approx 1$ mm and $\epsilon=11$, the voltage at the edge of the cluster $x=0.5$ μm is only 1/1000 of a percent smaller than in the center. For larger clusters of tens of micrometer length the deviations of the voltage from the center are bigger but still a small fraction of a percent. Hence for not extremely large sodium channel densities, we can assume that all sodium channels along a cluster are on an equipotential. For $\hat{l}\epsilon \ll 1$ and $\hat{l}\epsilon^2 \ll 1$, i.e., for small clusters with low density of sodium channels, the voltage at the center of the cluster, u_c, is given by

$$u_c \approx u_m + \frac{\epsilon^2 \hat{l}}{1+\left(\frac{g_m}{g_{\mathrm{Na}}}\right)}(u_{\mathrm{Na}}-u_m) \tag{10}$$

and is thus unsubstantially elevated from the base level u_m and action potentials will not be generated.

The outcome of this section is that the impedance coupling of the ion channels to the cable requires a large density of ion channels to be capable of raising the membrane potential enough to trigger an action potential. Effects of small numbers of ion channels can thus not be expected in a long axon or dendrite (i.e., a length of more than mm's). In order for small clusters with few sodium channels to generate action potentials and hence to exploit small cluster-size effects as we describe below, one has to place the ion channels onto a small piece of electrically isolated membrane with small impedance coupling to the channels.

In the opposite case of sodium channel clusters with large channel densities, like e.g., in the nodes of Ranvier, the parameter ϵ is larger. For a 2 μm cable and a node of Ranvier of 1 μm extent and 10^4 sodium channels, $\epsilon \approx 56$. Here, the potential at the center is only about 40% below the sodium reversal potential if all channels are open. Hence, the conductance of such a cluster is large enough to generate and hence conduct action potentials.

III. MODELING THE SODIUM CHANNEL CLUSTER

In light of the discussion in the previous section, we consider small clusters of sodium channels on small, electrically isolated domains. Although potassium channels contribute to the shape of the action potential they are not necessary to generate an action potential since sodium channels inactivate. The nodes of Ranvier, for example, comprise only voltage gated sodium channels.[14–16] The potassium channels present are not voltage-gated and thus represent leakage conductance. For the voltage dependence of the sodium conductance we use a stochastic Hodgkin-Huxley model with stripped potassium conductance but increased leakage conductance. As discussed above, voltage gradients within a cluster are extremely small and can be neglected and thus Eq. (1) becomes an ordinary stochastic differential equation for the membrane potential, i.e.,

$$\dot{u} = -\frac{g_m}{\bar{C}}(u-u_m) - n\frac{\gamma_{\mathrm{Na}}}{A\bar{C}}(u-u_{\mathrm{Na}}), \tag{11}$$

where A denotes the area of the cluster and n the number of open sodium channels. The sodium reversal potential and the leakage potential are given by $u_{\mathrm{Na}}=50$ mV and $u_m=-54.4$ mV. In order to mimic increased passive conductance, we decrease the membrane resistivity to 110 $\Omega\,\mathrm{cm}^2$ leading to a conductance of 9.1 $\mathrm{mS/cm}^2$ and to $\bar{C}/g_m=0.11$ ms.

The number of open sodium channels depends on the membrane potential. Each sodium channel has four gates that can be open or closed. Three identical, fast activation gates with opening and closing rates $\alpha_m(u)$ and $\beta_m(u)$

$$\alpha_m = \frac{0.1(50.0+u)}{1-\exp(-(50.0+u)/10.0)},$$
$$\beta_m = 4.0\exp\left(\frac{-u+75}{18.0}\right), \tag{12}$$

and one slow inactivation gate with opening and closing rates α_h and β_h, respectively,

$$\alpha_h = 0.07\exp(-(u+75)/20.0),$$
$$\beta_h = \frac{1.0}{\exp(-(45.0+u)/10.0)+1.0}, \tag{13}$$

determine the state of each channel. Note that we use the Hodgkin-Huxley expressions for the opening and closing rates with shifted voltages so that the resting voltage is about −65 mV. The reversal potentials are shifted accordingly. Only if all activation gates and the inactivation gate are open, the channel is conducting.

A stochastic simulation of the ion channels is necessary to determine the instantaneous number n of open sodium channels per cluster. We simulate the switching of the gates with Markov processes. If a gate is closed at time t, it will open within the time interval $[t,t+\delta t]$ with the probability $\alpha\delta t$ and remain closed with the probability $1-\alpha\delta t$. If a gate is open at time t, it will close with the probability $\beta\delta t$ within the time interval $[t,t+\delta t]$ and remain open with probability $1-\beta\delta t$. This method, although accurate, is numerically very inefficient since many simulated transitions between channel states have no consequences for the conductance of the cluster and for large ion channel clusters better methods are advisable (see, e.g., Ref. 11, and references therein). The stochastic opening and closing of sodium channels results in fluctuations of the membrane potential and if these fluctuations are large enough in spontaneous action potentials. We are interested in how the rate of these action potentials depends on the number of channels in the cluster.

A. Spontaneous action potentials

Denoting the number density of sodium channels by ρ_{Na}, the membrane surface area of the cluster can be expressed as $A=N/\rho_{\mathrm{Na}}$, where N is the total number of sodium channels in the cluster. Inserting this expression into Eq. (11) yields for

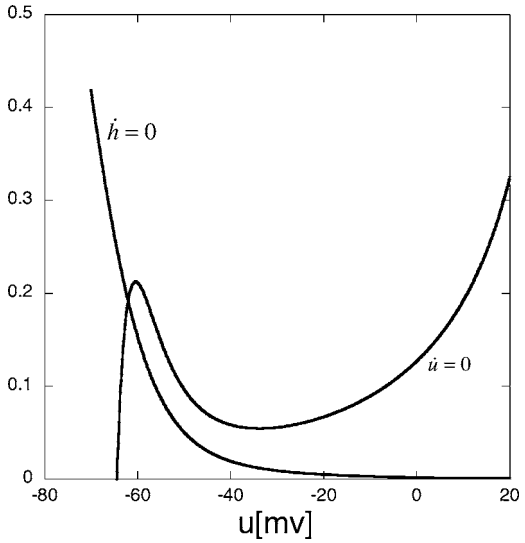

FIG. 1. The null clines $\dot{h}=0$ and $\dot{u}=0$ are shown as a function of the membrane potential.

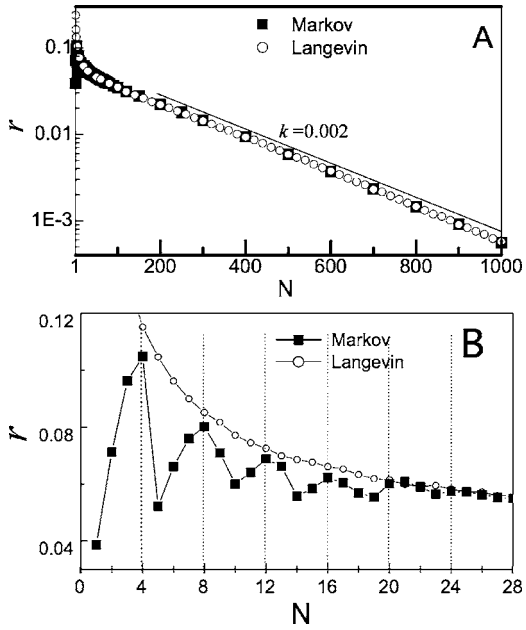

FIG. 2. We show the rate of the action potentials of the sodium channel cluster for a large range of cluster sizes (A), and for small sizes (B) obtained through Markov modeling (solid squares) and the Langevin approach (open circles).

the term describing sodium conductance $-(n/N)(\gamma_{\mathrm{Na}}\rho_{\mathrm{Na}}/\bar{C})\times(u-u_{\mathrm{Na}})$. The first factor (n/N) describes the fraction of open channels in the cluster. For now, we simplify the gating dynamics by replacing the fraction of channels with open (fast) activation gates by their steady-state value, i.e., $(\alpha_m/(\alpha_m+\beta_m))^3$ and only consider the slow opening and closing of the inactivation gates stochastically. The simplified equation for the membrane potential reads

$$\dot{u}=-\frac{g_m}{\bar{C}}(u-u_m)-\left(\frac{n}{N}\right)\left(\frac{\alpha_m}{\alpha_m+\beta_m}\right)^3\frac{\gamma_{\mathrm{Na}}\rho_{\mathrm{Na}}}{\bar{C}}(u-u_{\mathrm{Na}}), \qquad (14)$$

where (n/N) now describes the fraction of noninactivated channels.

In the limit of large clusters, i.e., $N\to\infty$, the fraction (n/N) assumes continuous values h on the unit interval and the master equation governing the number of activated channels n reduces to the rate equation[12]

$$\dot{h}=\alpha_h(1-h)-\beta_h h. \qquad (15)$$

The combination of Eqs. (14) and (15) determines the dynamics of the system. The null clines ($\dot{u}=0$, $\dot{h}=0$) are shown in Fig. 1. The null clines intersect at a single point which is a stable fixed point rendering the system excitable. In order to fire an action potential, the variable h has to exceed a threshold, which is somewhat larger than the maximum value of the null cline $g_1(u)$ because the dynamics of u is not instantaneous. Numerical calculations yield a threshold value of $h=0.24$ for the parameters used here. Hence, in order to fire an action potential a fraction of at least 24% of sodium channels need to be open. When the voltage reaches its maximum, the sodium channels inactivate, the fraction of activated channels drops suddenly below resting value, and consequently the voltage drops and the action potential is terminated.

If the number of sodium channels per cluster decreases, the fraction of open channels n/N can change by discrete amounts $1/N$ causing discrete, stochastic changes in the sodium conductance and hence voltage fluctuations. These fluctuations can cause action potentials by chance which can be characterized by simple measures like the mean stochastic firing rate or fluctuations of the time intervals in between two subsequent spikes.

B. Stochastic spiking rate and magic cluster sizes

For large numbers of channels, i.e., weak fluctuations, stochastic spikes occur when h exceeds a threshold. This activation process is expected to be characterized by a spiking rate $r(N)$ that decreases exponentially with decreasing noise strength and hence increasing system size N, i.e.,

$$r(N)\propto\exp(-kN). \qquad (16)$$

Simulations using the above described Markov-process method [see Fig. 2(A)] confirms this hypothesis with an exponent of $k=0.002$ for *large* sodium channel clusters. For small numbers of channels per cluster, however, we observe distinct deviations from this large N asymptotics with peaks and valleys [see Fig. 2(B)]. In the following we will explore the origin of these peaks and valleys. To this end it is instructive to plot some samples of the simulated trajectories in Fig. 3 for different cluster sizes. For $N=4$ (B), there are clearly the most spikes, more than, e.g., for $N=5$. However, there are more events with two channels open for $N=5$ than for $N=4$. This observation gives us the important clue that the number of channels required to be open in order to generate a spike must be different for $N=4$ and $N=5$. Given the threshold of $h=0.24$ (see above), the necessary fraction of open channels in order to generate an action potential is indeed 2 for $N=5$ since $1/5=0.2<0.24$ and 1 for $N=4$ since $1/4=0.25>0.24$. This also explains the drop in the firing rate from $N=4$ to $N=5$.

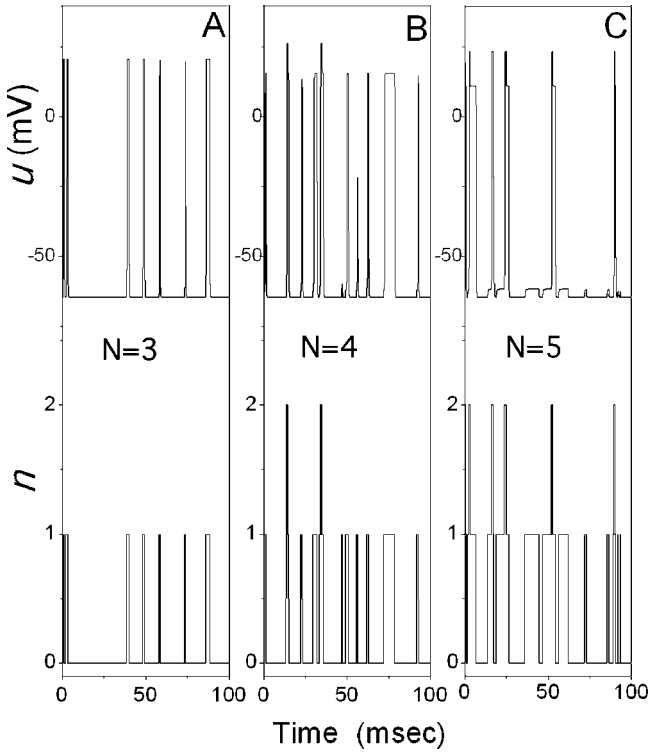

FIG. 3. Stochastic trains of action potentials (upper panel) and the corresponding number of open channels n (lower panel) are shown for $N=3$ (A), $N=4$ (B), and $N=5$(C).

We can now further elaborate on this idea to explain all peaks and valleys in Fig. 2(B). The cluster state can be characterized in terms of the number of open channels, i.e., 0 channels open, 1 channel open, 2 channels open, etc. We further assume that we cannot distinguish between individual channels and that all states have the same probability. This latter *microcanonical* assumption is not correct since the membrane voltage changes with the number of open channels modifying the opening and closing rates and hence the opening probabilities. Nevertheless this theory, although an approximation, captures the underlying mechanism for the peaks and valleys very well and we present it here. If for instance the cluster is comprised of $N=3$ channels, the states of the cluster with $n=1$, 2 or 3 h open channels are states that can trigger an action potential because of $n/N>0.24$ for these three states. Thus three out of all four possible h open states are associated with an action potential. Similarly, if the cluster is comprised of four channels, 4/5 of all possible states are associated with an action potential since $1/4>0.24$. Since there are more states associated with the firing state (i.e., $4/5>3/4$), the probability of firing and thus the firing rate is increased as N increased from 3 to 4, as can be seen in the upper panel of Fig. 3. If, however, the cluster comprises five channels only 4/6 of all h open states are associated with an action potential since now at least two channels need to be h activated ($2/5>h_{\min}=0.24$). The fraction of the numbers of states of the channel cluster associated with an action potential, drops as the cluster size is increased from 4 to 5 from 0.8 to 2/3. As a consequence, the firing rate drops to a lower level as N is increased from 4 to 5.

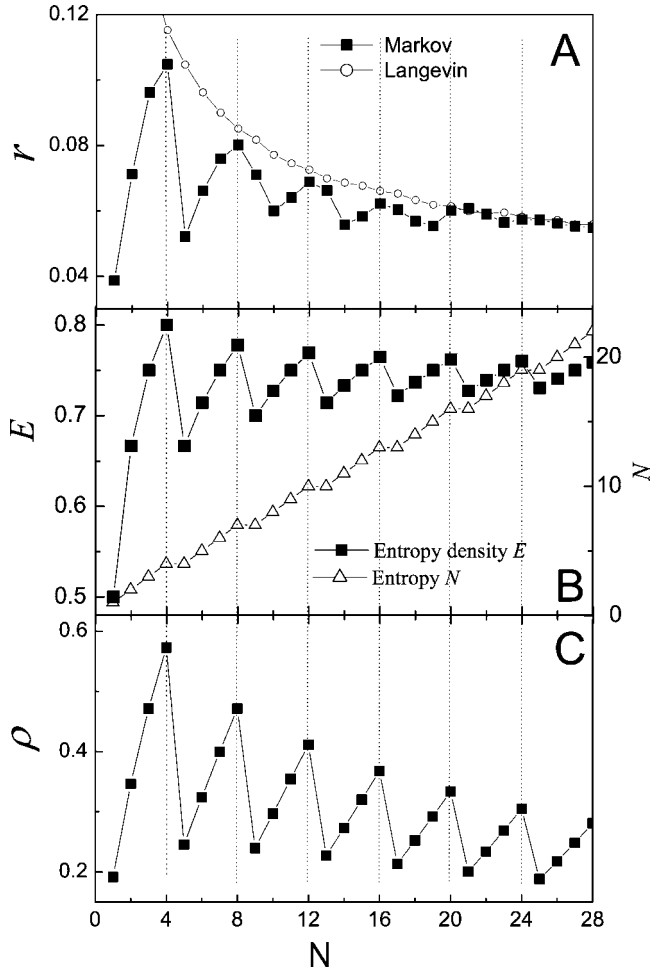

FIG. 4. (A) The spontaneous firing rate r as a function of the cluster size N of sodium channels for small clusters. The firing rate obtained with the accurate Markov process (solid squares) are compared with those obtained from the approximative Langevin equation (open circle). The entropy e and the entropy density E (B), and the combinatorial probability ρ at $h_{\min}=0.24$ are shown for comparison (C). The maxima of the firing rate coincide well with maxima both in the entropy density and the combinatorial probability.

If we had assumed that the channels are distinguishable and had counted the number of ways a certain number of channels can be open, we had arrived at 28/32 for $N=3$, 30/32 for $N=4$ and 26/32 for $N=5$ with a maximum at $N=4$.

We now generalize this analysis for a cluster of N sodium channels under the microcanonical assumption and that the channels are indistinguishable. Algebraically this boils down to calculating the fraction of all fractions $0/N, 1/N, 2/N, \ldots, N/N$ with values above the threshold $h_{\min}$, i.e.,

$$E(N,\ h_{\min}) = (N - \text{integer}(Nh_{\min}))/(N+1), \tag{17}$$

which we term the entropy density of the cluster. The entropy density $E(N,\ h_{\min})$ is plotted in Fig. 4 and indeed shows maxima at exactly those system sizes where the rate exhibits maxima. The entropy $e=E(N,\ h_{\min})(N+1)$ also shown in Fig. 4 exhibits plateaus where the entropy density exhibits peaks. If we had assumed that the channels were distinguishable, the result would have been

$$E(N,\ h_{\min}) = 1 - 2^{-N}\left(1 + \sum_{k=1}^{\mathrm{int}(h_{\min}N)} \binom{N}{k}\right), \tag{18}$$

with peaks at the same N than in Eq. (17).

Although the microcanonical theory presented above captures the observed effect of multiple peaks quite well, it is not entirely accurate since not all states do have the same probability. It is, for example, less likely that all N channels are open simultaneously then one channel or no channel is open [see Figs. 3(A)–3(C)]. In the following we sketch a more accurate theory that goes beyond the microcanonical counting. At a given voltage u, the probability that n of the N sodium channels are activated and thus the other $N-n$ channel are inactivated is given by the binomial distribution,

$$P(n,N) = \binom{n}{N} p_o^n(u_0) p_c^{(N-n)}(u_0), \tag{19}$$

where

$$p_o = \frac{\alpha_h(u)}{\alpha_h(u) + \beta_h(u)}, \quad p_c = 1 - p_o. \tag{20}$$

We replace the voltage u by the resting potential $u_0 = -65$ mV, obtained from Eq. (14). The constant resting voltage u_0 is a good approximation as most of the slow inactivation changes occur prior to the action potential where the deviation of the voltage from the resting values are typically small. The sum of the probabilities P for all the states which associate with an action potential, i.e., the states in which the fraction of open channels are larger than or equal to $h_{\min}$, is defined as the combinatorial probability ρ,

$$\rho = \sum_{n=n_{\min}}^{N} P(n,N), \tag{21}$$

with $n_{\min} = \mathrm{int}(h_{\min}N) + 1$. The combinatorial probability $\rho(N)$ is calculated numerically at $h_{\min} = 0.24$ as a function of cluster size N and plotted in Fig. 4(C). One can see that the combinatorial probability exhibits peaks at exactly the same system sizes as the entropy density of the microcanonical theory and the spiking rate r. Although the combinatorial theory is more accurate, it does not generate the insight into the multiple peak effect as well as the phenomenological treatment.

To further confirm our hypothesis that the observed peaks and valleys in the spontaneous spiking rate are due to the *discrete nature* of small inverse integers and not some other effect like stochastic resonance, we approximate the exact Markov process describing the dynamics of the channels by a Langevin equation which is *continuous* in the fraction of open channels h. Such an approach has been put forward by Fox and Lu[13] (see also Refs. 1, 17, and 18) and the Langevin equations read

$$\begin{aligned} \frac{du}{dt} &= \frac{1}{\tau_{\mathrm{Na}}} m_\infty^3(u) h (u_{\mathrm{Na}} - u) + \frac{1}{\tau_{\mathrm{leak}}}(u_{\mathrm{leak}} - u), \\ \frac{dh}{dt} &= \alpha_h(1-h) - \beta_h h + G_h(t), \end{aligned} \tag{22}$$

where $G_h(t)$ denotes zero-mean, uncorrelated, Gaussian white-noise terms with

$$\langle G_h(t) G_h(t') \rangle = \frac{\alpha_h(1-h) + \beta_h h}{N} \delta(t - t'). \tag{23}$$

The Langevin approach treats the stochastic dynamics of the clustered channels as deterministic dynamics disturbed by Gaussian white noise. The open circles in Fig. 2(B) represent the results obtained by simulating Eqs. (22) and (23). Although the overall behavior agrees quite well for the plotted range of cluster sizes, it does not reproduce the peaks and valleys.

Most of the insight into the nature of these peaks can be obtained from the simple microcanonical counting theory. It is the entropy density of the firing state of the ion channel cluster, i.e., the fraction of all cluster states in which action potentials are fired, that exhibits peaks and valleys as the system size is increased. The key for this behavior is the sharp firing threshold for the fraction of open channels in conjunction with the discreteness of inverse small integers $1/N,\ 2/N, \ldots$. This threshold, however, is generated by the fast gates of the sodium channels which we modeled nonstochastically. It is therefore a critical question whether the firing rate exhibits peaks and valleys for a fully stochastic model as well.

C. Stochastic spiking rate in the fully stochastic model for the sodium channels

In the system we studied above, we only considered the slow inactivation dynamics of the sodium channel stochastically. In a fully stochastic model for the sodium channels, also the fast gates have to be modeled stochastically using a Markov approach. Each channel now has four stochastic gates with the opening and closing rates given in Eqs. (12) and (13). A channel is open only if all three activation gates m and the inactivation gate h are open. The fraction of open states n/N, calculated through simulations of Markov processes, enters in the differential equation for the membrane potential, i.e.,

$$\dot{u} = -\frac{g_m}{\bar{C}}(u - u_m) - \frac{n}{N}\frac{\gamma_{\mathrm{Na}}\rho_{\mathrm{Na}}}{\bar{C}}(u - u_{\mathrm{Na}}), \tag{24}$$

where (n/N) denotes the fraction of open channels. In Figs. 5(A) and 5(B) we show a short train of spikes and the corresponding number n of open channels at a system size of $N=20$. In comparison to the reduced model studied above, the action potential amplitudes exhibit more variation although in the macroscopic limit (at large system sizes) both models behave almost identical. From Figs. 5(A) and 5(B), one can see that each action potential amplitude is associated with a unique number of open sodium channels. The larger the action amplitude, the larger the fraction of open channels

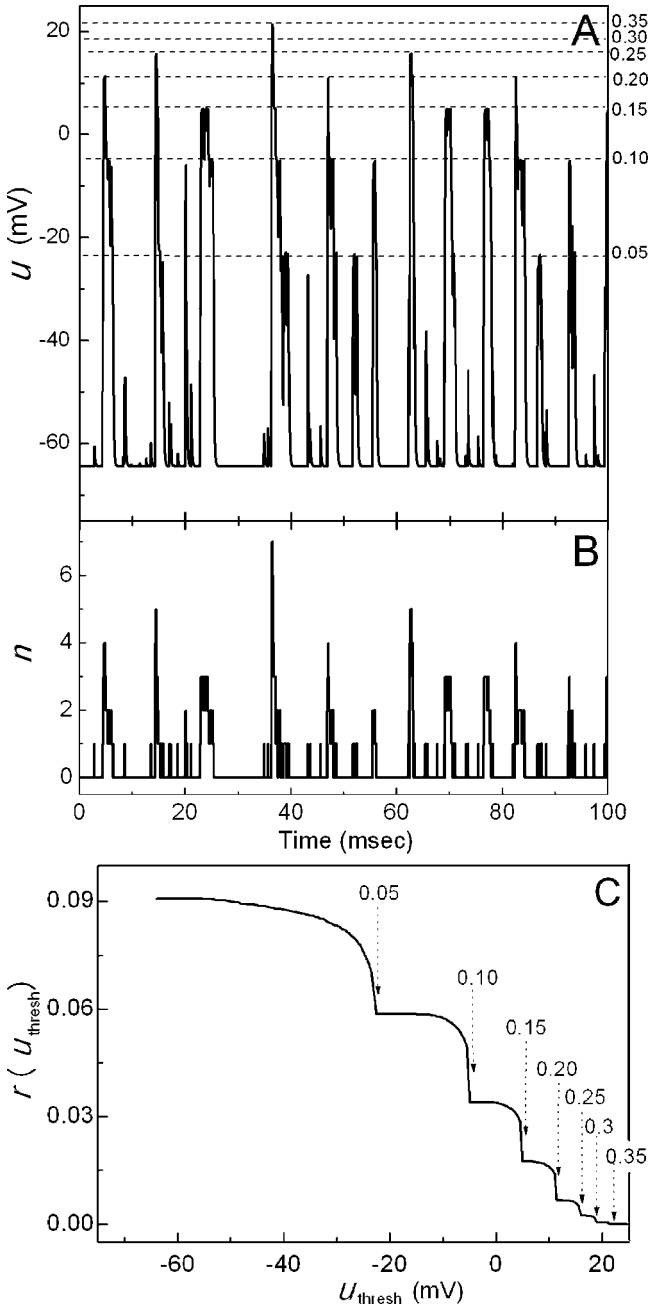

FIG. 5. (A) A short spike train generated by the stochastic model described by Eq. (24) and (B) the corresponding number of open channels are shown for a cluster of 20 sodium channels. Each action potential amplitude is associated with a certain fraction of open channels. The respective fraction of open channels is annotated at the right end of the dashed lines. (C) The cumulative rate of action potentials as a function of the amplitude threshold u_{thresh} for action potentials. A big drop of the spiking rate is seen at threshold voltages that are steady-state voltages for a certain fraction of open channels n/N (annotated by the dotted arrow with the respective fraction of open channels).

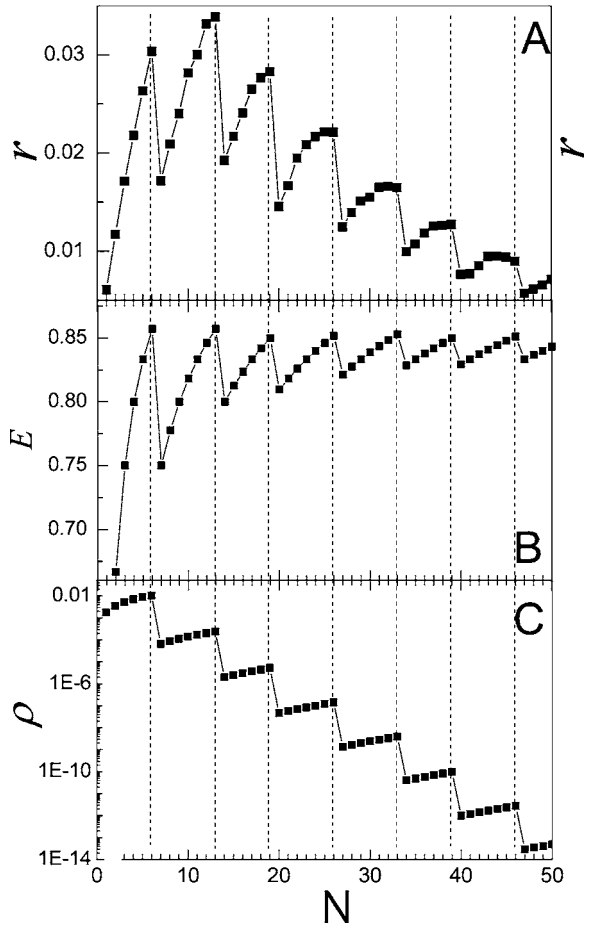

FIG. 6. (A) The spontaneous spiking rate of action potentials with amplitude larger than (or equal) 5.0 mV is compared to the entropy density $E(N,h_{\min}=0.15)$ (B) and the combinatorial probability ρ (C), as a function of system size N.

n/N. The relation of action potential amplitude and fraction of open channels can be determined by calculating the steady-state voltages u_{ss} of Eq. (24) for a fixed n/N [dashed lines in Fig. 5(A)]. For example, $u_{\text{ss}}=5$ mV is obtained for $n/N=0.15$.

The consequence of the variability of amplitudes is that for different amplitude thresholds different spiking rates are found. The cumulative firing rate, i.e., the rate of action potentials with amplitudes of at least u_{thresh} is shown for a cluster of 20 sodium channels in Fig. 5(C) as a function of u_{thresh}. Generally, a lower amplitude threshold corresponds to a larger spiking rate, but Fig. 5(C) also shows that the spiking rate changes rapidly around the steady voltages $u_{\text{ss}}(n/N)$ at a given fraction of open channels, but changes slowly between two successive steady-state voltages. This observation confirms that the action potential amplitudes are distributed somewhat discretely around the steady voltages $u_{\text{ss}}(n/N)$. The rate of spontaneous action potentials $r(N,u_{\text{thresh}})$ with an amplitude of at least $u=u_{\text{thresh}}=5$ mV is shown as a function of the cluster size N in Fig. 6(A). Similar to the reduced model above, the spiking rate exhibits a series of peaks at multiple cluster sizes. These system sizes, however, now depend on the threshold amplitude u_{thresh}, since the minimum fraction of open channels necessary to generate such a spike depends on u_{thresh}. The threshold amplitude $u_{\text{thresh}}=5$ mV represents the steady voltage determined from Eq. (24) when 15% of the channels are open [compare Fig. 5(A)]. Applying Eq. (17) with $h_{\min}=0.15$ (corresponding to $u_{\text{thresh}}=5$ mV) we obtain the entropy density E shown in Fig. 6(B). Maxima of the firing rate coincide well with maxima in the entropy density $E(N,h_{\min}=0.15)$.

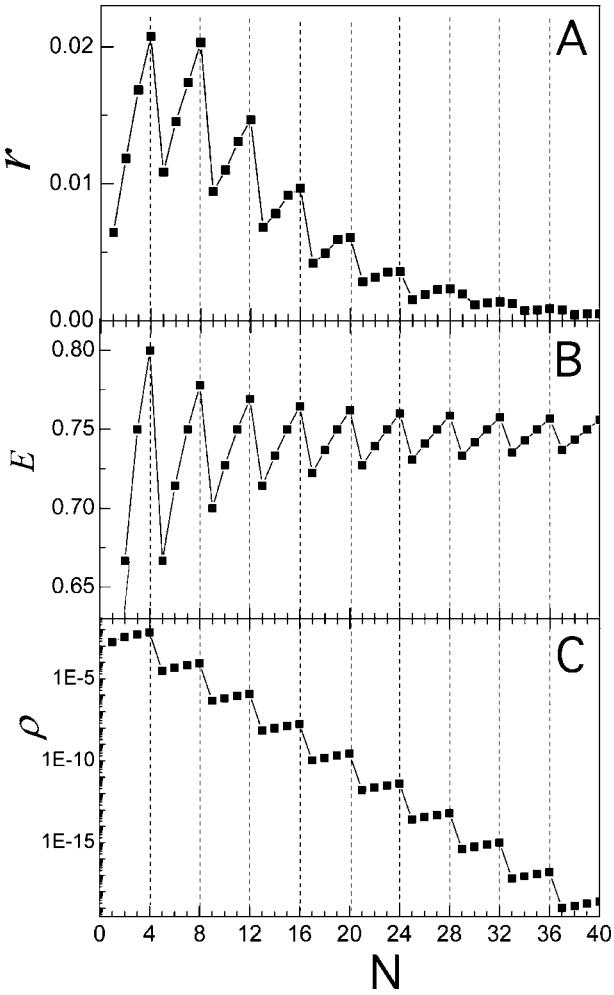

FIG. 7. (A) The spontaneous spiking rate of action potentials with amplitude larger than (or equal) 15.0 mV is compared to the entropy density $E(N,h_{\min}=0.249)$ (B) and the combinatorial probability ρ (C), as a function of the cluster size N.

The combinatorial probability ρ Eq. (21) with $P(n,N)$ given in Eq. (19) can be determined with the modified open probability

$$p_o = \frac{\alpha_h(u)}{\alpha_h(u)+\beta_h(u)}\left(\frac{\alpha_m(u)}{\alpha_m(u)+\beta_m(u)}\right)^3 \tag{25}$$

which reflects that n/N is now the true fraction of open channels and not the fraction of noninactivated channels (as in the reduced model). We again approximate u by the resting potential of −65 mV since the voltage changes are small prior to an action potential. For a threshold of $h_{\min}=0.15$, the combinatorial probability ρ is shown as a function of the cluster size in Fig. 6(C). Although the absolute value of the combinatorial probability becomes quite small with increasing N, the maxima in the combinatorial probability ρ coincide well with the maxima of the firing rate r.

Similarly, good agreement between the maxima of the firing rate and those of the E and ρ is obtained for other voltage thresholds. In Figs. 7(A)–7(C) we depict the firing rate (A), the entropy-like density E (B) and the combinatorial probability ρ (C) for a voltage threshold of $u_{\text{thresh}}=15$ mV, corresponding to a fraction of open channels of $n/N=0.25$.

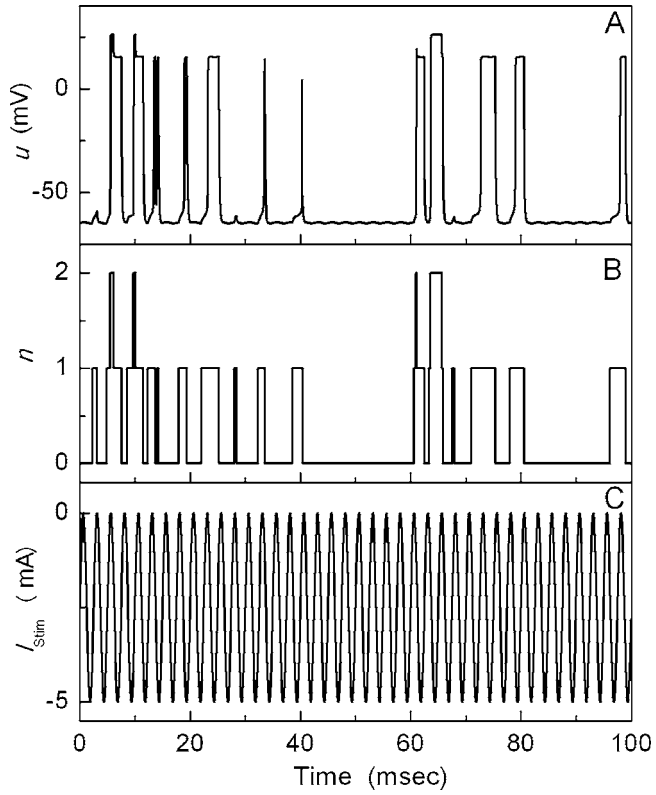

FIG. 8. Stochastic spike trains (A) and the corresponding number of open channels (B) for a cluster of $N=4$ sodium channels with a periodic current with amplitude $I_0=2.5$ and frequency $\nu_0=0.4$ Hz.

D. Entropically enhanced response to an external signal

The response of the noisy excitable system to an external periodic signal has been studied extensively in the context of stochastic resonance.[8] There, an optimally chosen level of noise can enhance the coding of a weak subthreshold signal.

In this section, we will show that the response of ultrasmall clusters of sodium channels to an external signal shows—similar to the spontaneous firing rate—a surprisingly rich structure with peaks and valleys as the cluster size is changed. This structure—as the firing rate above—can be traced back to the discreteness of inverse integers. The signal is represented by an externally injected current

$$I_{\text{stim}} = -I_0 + I_0 \sin(2\pi\nu_0 t), \tag{26}$$

added to the equation for the membrane voltage. Similar results as those we present below can be obtained if, instead of adding a periodic current, the sodium conductance is modulated periodically, mimicking periodic binding and unbinding of neurotransmitters to receptors and subsequent opening of sodium channels.

The modulation function is chosen such that it leaves the minimum excitation threshold unchanged and independent of the amplitude I_0. As an example we show a train of voltage spiked and the corresponding number of open channels in Fig. 8 for a cluster of $N=4$ sodium channels, responding to a periodic signal with an amplitude of $I_0=2.5$ and a frequency of $\nu_0=0.4$ Hz. One can see that the action potentials [Fig.

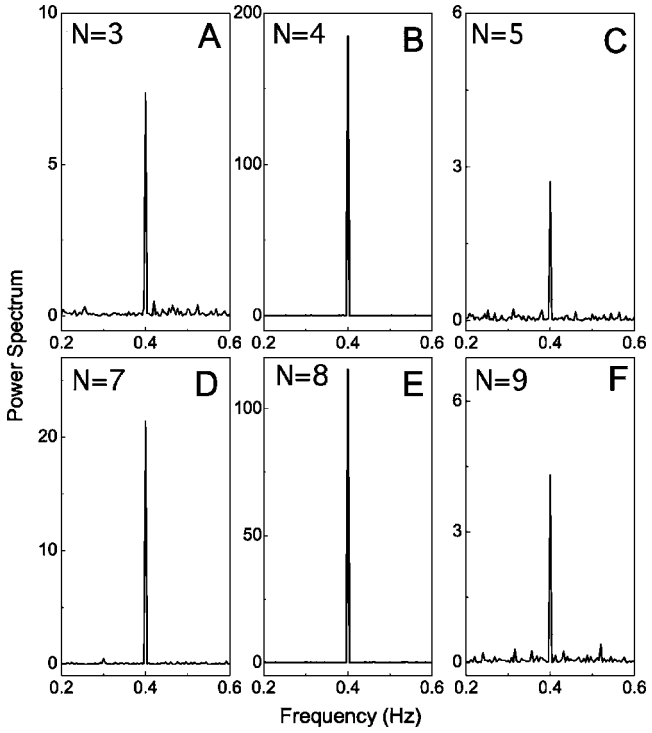

FIG. 9. The power spectra of the system responding to an external periodic current are plotted at size of (A) $N=3$, (B) $N=4$, (C) $N=5$, (D) $N=7$, (E) $N=8$, and (F) $N=9$. Here $I_0=2.5$, $\nu=0.4$ Hz for the signal. Please note that the scales of the y axis are different for these subfigures. The peak amplitudes of power spectrum increase to 185 and 115 for $N=4$ and $N=8$, respectively.

8(A)] are initiated most frequently when the external stimulus $I_{\text{stim}}(t)$ approaches its maximum at $I_{\text{stim}}=0$ [Fig. 8(C)].

In order to assess the encoding of the periodic current we calculate the power spectrum of the spike train generated by the system where the spikes are approximated by δ functions at the spike times t_n, i.e.,

$$S(\nu) = \lim_{T\to\infty} \frac{1}{T} \left| \int_0^T \sum_n \delta(t-t_n)\exp(-2i\pi\nu t)dt \right|^2$$

$$= \lim_{T\to\infty} \frac{1}{T} \left| \sum_n \exp(-2i\pi\nu t_n) \right|^2, \quad (27)$$

where T is the total length of the spike train. We have solved Eq. (14) for the membrane potential in conjunction with a Markov simulation of the states of the ion channels with the additional current in Eq. (26). The corresponding power spectra are shown in Fig. 9 for clusters with $N=3$, 4, 5, 7, 8, and 9 channels. Each power spectrum exhibits a sharp peak at the frequency of the signal (see Ref. 8), with a weight representing the encoding of the signal in the spike train. One can see from Fig. 9 that the signal encoding w (weight of the signal peak in the power spectrum of the spike train) exhibits maxima at $N=4$ and 8. The weight of the signal peak at the signal frequency of ν_0 is plotted in Fig. 10 as a function of the cluster size obtained with both, the Markov method and Langevin approach Eqs. (22) and (23). Since the signal is subthreshold it is not surprising that we find stochastic resonance-like behavior where the cluster size N is inversely proportional to noise strength[1–3] with the

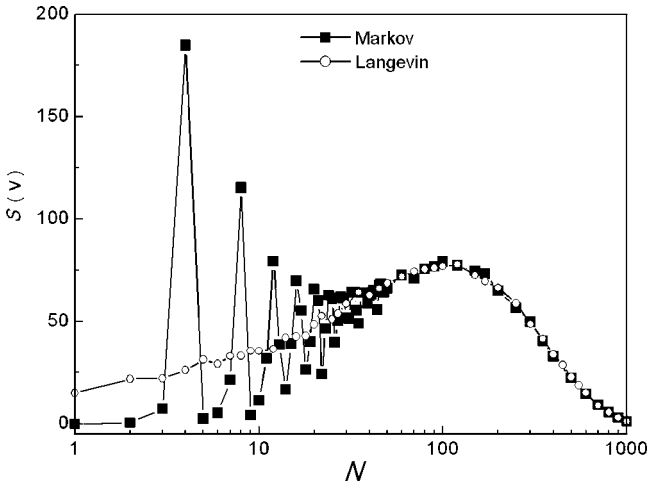

FIG. 10. Encoding ability $S(\nu)$ of the system responding to the periodic current at $I_0=2.5$, $\nu=0.4$ Hz as a function of the system size from $N=1$ to 1000. The results are obtained with both the Markov process (solid squares) and Langevin approach (open circles).

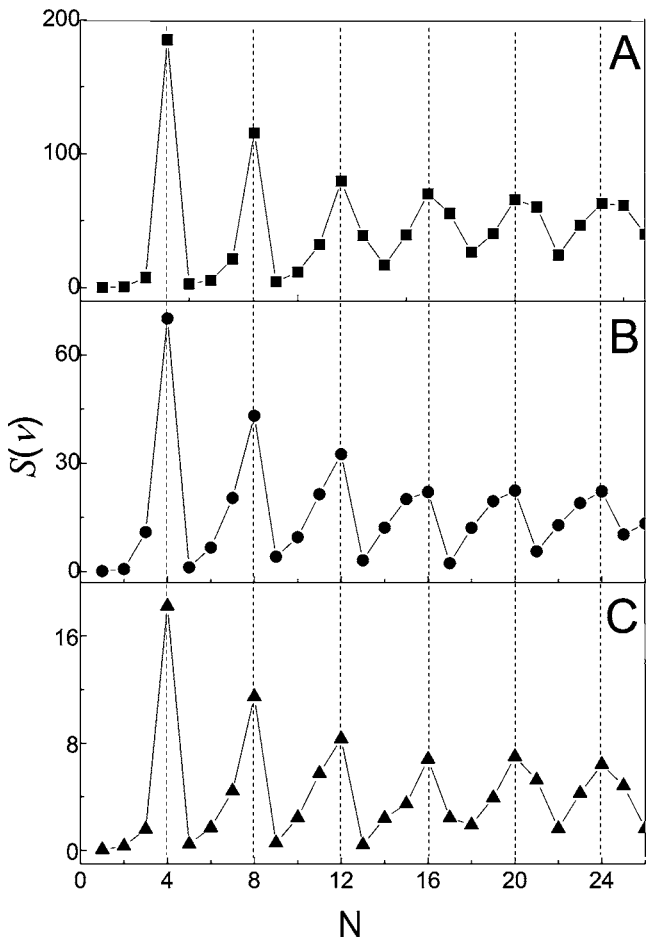

FIG. 11. Encoding ability $S(\nu)$ of the system responding to the periodic current as a function of the system size from $N=1$ to 26, for (A) $I_0=2.5$, $\nu=0.4$ Hz (squares), (B) $I_0=2.0$, $\nu=0.8$ Hz (circles), and (C) $I_0=1.0$, $\nu=0.8$ Hz (triangles). These three curves show the peaks at the same system sizes.

Langevin approach. What is most interesting are the additional sharp peaks in the signal encoding only obtained with the Markov approach, indicating again that it is the discreteness of inverse small integers causing these peaks. The encoding ability w is plotted in Fig. 11 for a range of small cluster sizes and various signal amplitudes. For *all* amplitudes, we find multiple maxima at cluster sizes which coincide with those where the spontaneous firing rate in the absence of the periodic signal (see Fig. 4) showed maxima. Furthermore, Fig. 11 indicates that the peaks of the weights w are not sensitive to variations in the signal frequency ν_0 either. Thus, clustered ion channels encode periodic signals with a wide range of frequencies and amplitudes most efficiently at certain specific magic cluster sizes. As shown in Fig. 8, the action potentials are induced most frequently around the maximum of external stimulus, i.e., at $I_{\mathrm{stim}}=0$. The encoding ability w is thus mainly determined by the spiking rate r at $I_{\mathrm{stim}}=0$ [Fig. 4(A)]. The spiking rate $r(N)$, in turn, shows maxima when the entropy density $E(N)$ given in Eq. (17) exhibits maxima. As a result, the peaks of the signal encoding w of the clustered channels (Fig. 11) is determined by the entropy density or equivalently by the combinatorial probability [Figs. 4(B) and 4(C)]. In brief, it is the enhanced sampling of the signal at certain cluster sizes that aids in enhancing the encoding.

IV. DISCUSSION AND CONCLUSIONS

Small clusters of sodium channels embedded in a leaky membrane with a realistic resistivity can generate electrically excitable behavior if they are embedded in a *small* patch of membrane. We have shown in Sec. I, that if the channels are embedded in an infinite cable, it requires thousands of channels to provide enough current to charge the membrane capacitance. Thus, effects of the smallness of an excitable system are not observable electrically unless a small patch of a membrane is used. We also have shown that voltage gradients can be neglected within channel clusters since the typical electrical length scale is of the order of hundreds of μm unless very large densities of channels are present. We consider electrically isolated sodium channel clusters with constant channel densities as a function of the cluster size. The channel density we chose, i.e., $60/\mu\mathrm{m}^2$ is consistent with the Hodgkin-Huxley sodium conductance. Hence a cluster of 5 channels is embedded in an membrane area of $0.0833\ \mu\mathrm{m}^2$. The capacitance of such a patch of membrane is about 8.3×10^{-4} pF and holds only about 300 singly charged ions. To change the membrane potential by 100 mV requires moving of only about 520 singly charged ions. Given a sodium channel conductance of about 20 pS, the current at a membrane potential of 60 mV is about 1 pA. Within the time scale of 1 ms this allows about $5000\gg520$ singly charged ions to pass the channels, i.e., enough to elicit an action potential. We report that clusters of that size do exhibit some novel features, i.e., maximal spiking rates and signal encoding at specific cluster sizes, that are fundamental for the biophysical nature of the problem. Signals are encoded optimally regardless of frequency and amplitude. An important condition for these effects to occur is a one-to-one quasidiscrete relation between the fraction of open channels and the membrane potential. This limits the effect to homogeneous channel clusters with a relatively simple gating dynamics. The full Hodgkin-Huxley model including the potassium channels does not exhibit peaks in the firing rate or signal encoding since there are many configurations of open sodium and potassium channels with a similar membrane potential.

[1] G. Schmid, I. Goychuk, and P. Hanggi, Europhys. Lett. **56**, 22 (2001).
[2] P. Jung and J. W. Shuai, Europhys. Lett. **56**, 29 (2001).
[3] A. Pikovsky, A. Zaikin, and M. A. de la Casa, Phys. Rev. Lett. **88**, 050601 (2002).
[4] J. W. Shuai and P. Jung, Phys. Rev. Lett. **88**, 068102 (2002).
[5] A. Zaikin, J. Garcia-Ojalvo, R. Bscones, E. Ullner, and J. Kurths, Phys. Rev. Lett. **90**, 030601 (2003).
[6] J. W. Shuai and P. Jung, Phys. Rev. Lett. **95**, 114501 (2005).
[7] Y. Tateishi, M. Hattori, T. Nakayama, M. Iwai and H. Bannai and T. Nakamura, T. Michikawa, T. Inoue, and K. Mikoshiba, J. Biol. Chem. **280**, 6816 (2005).
[8] L. Gammaitoni, P. Hanggi, P. Jung, and F. Marchesoni, Rev. Mod. Phys. **70**, 223 (1998).
[9] J. W. Shuai and P. Jung, Proc. Natl. Acad. Sci. U.S.A. **100**, 506 (2003).
[10] J. Sneyd and J. Keener, *Mathematical Physiology* (Springer Verlag, Berlin, 1998).
[11] C. Koch, *Biophysics of Computation* (Oxford University Press, Oxford, 1999).
[12] C. W. Gardiner, *Handbook of Stochastic Methods* (Springer, Berlin, 1983).
[13] R. F. Fox and Y. N. Lu, Phys. Rev. E **49**, 3421 (1994).
[14] A. L. Hodgkin and A. F. Huxley, J. Physiol. (London) **117**, 500 (1952).
[15] P. Shrager, J. Physiol. (London) **404**, 695 (1988).
[16] B. Hille, *Ion Channels of Excitable Membranes* (Sinauer Associates, Dunderland, 2001).
[17] G. Schmid, I. Goychuk, and P. Hanggi, Physica A **325**, 165 (2003).
[18] G. Schmid, I. Goychuk, and P. Hanggi, Phys. Biol. **1**, 61 (2004).